

# First observation of new isomers in $^{228}\text{Ac}$ : Impact on dark matter searches

K. W. Kim,<sup>1</sup> G. Adhikari,<sup>2</sup> E. Barbosa de Souza,<sup>3</sup> N. Carlin,<sup>4</sup> J. J. Choi,<sup>5</sup> S. Choi,<sup>5</sup> M. Djamal,<sup>6</sup> A. C. Ezeribe,<sup>7</sup> L. E. França,<sup>4</sup> C. Ha,<sup>8</sup> I. S. Hahn,<sup>9, 10, 11</sup> E. J. Jeon,<sup>1</sup> J. H. Jo,<sup>3</sup> H. W. Joo,<sup>5</sup> W. G. Kang,<sup>1</sup> M. Kauer,<sup>12</sup> H. Kim,<sup>1</sup> H. J. Kim,<sup>13</sup> S. H. Kim,<sup>1</sup> S. K. Kim,<sup>5</sup> W. K. Kim,<sup>11, 1</sup> Y. D. Kim,<sup>1, 14, 11</sup> Y. H. Kim,<sup>1, 15, 11</sup> Y. J. Ko,<sup>1, \*</sup> E. K. Lee,<sup>1</sup> H. Lee,<sup>11, 1</sup> H. S. Lee,<sup>1, 11, †</sup> H. Y. Lee,<sup>1</sup> I. S. Lee,<sup>1</sup> J. Lee,<sup>1</sup> J. Y. Lee,<sup>13</sup> M. H. Lee,<sup>1, 11</sup> S. H. Lee,<sup>11, 1</sup> S. M. Lee,<sup>5</sup> D. S. Leonard,<sup>1</sup> B. B. Manzato,<sup>4</sup> R. H. Maruyama,<sup>3</sup> R. J. Neal,<sup>7</sup> S. L. Olsen,<sup>1</sup> B. J. Park,<sup>11, 1</sup> H. K. Park,<sup>16</sup> H. S. Park,<sup>15</sup> K. S. Park,<sup>1</sup> R. L. C. Pitta,<sup>4</sup> H. Prihtiadi,<sup>1</sup> S. J. Ra,<sup>1</sup> C. Rott,<sup>17</sup> K. A. Shin,<sup>1</sup> A. Scarff,<sup>7</sup> N. J. C. Spooner,<sup>7</sup> W. G. Thompson,<sup>3</sup> L. Yang,<sup>2</sup> and G. H. Yu<sup>17</sup>

(COSINE-100 Collaboration)

<sup>1</sup>Center for Underground Physics, Institute for Basic Science (IBS), Daejeon 34126, Republic of Korea

<sup>2</sup>Department of Physics, University of California San Diego, La Jolla, CA 92093, USA

<sup>3</sup>Department of Physics and Wright Laboratory, Yale University, New Haven, CT 06520, USA

<sup>4</sup>Physics Institute, University of São Paulo, 05508-090, São Paulo, Brazil

<sup>5</sup>Department of Physics and Astronomy, Seoul National University, Seoul 08826, Republic of Korea

<sup>6</sup>Department of Physics, Bandung Institute of Technology, Bandung 40132, Indonesia

<sup>7</sup>Department of Physics and Astronomy, University of Sheffield, Sheffield S3 7RH, United Kingdom

<sup>8</sup>Department of Physics, Chung-Ang University, Seoul 06973, Republic of Korea

<sup>9</sup>Department of Science Education, Ewha Womans University, Seoul 03760, Republic of Korea

<sup>10</sup>Center for Exotic Nuclear Studies, Institute for Basic Science (IBS), Daejeon 34126, Republic of Korea

<sup>11</sup>IBS School, University of Science and Technology (UST), Daejeon 34113, Republic of Korea

<sup>12</sup>Department of Physics and Wisconsin IceCube Particle Astrophysics Center, University of Wisconsin-Madison, Madison, WI 53706, USA

<sup>13</sup>Department of Physics, Kyungpook National University, Daegu 41566, Republic of Korea

<sup>14</sup>Department of Physics, Sejong University, Seoul 05006, Republic of Korea

<sup>15</sup>Korea Research Institute of Standards and Science, Daejeon 34113, Republic of Korea

<sup>16</sup>Department of Accelerator Science, Korea University, Sejong 30019, Republic of Korea

<sup>17</sup>Department of Physics, Sungkyunkwan University, Suwon 16419, Republic of Korea

(Dated: May 24, 2022)

We report the discovery of two metastable isomeric states of  $^{228}\text{Ac}$  at 6.28 keV and 20.19 keV, with lifetimes of  $299 \pm 11$  ns and  $115 \pm 25$  ns, respectively. These states are produced by the  $\beta$ -decay of  $^{228}\text{Ra}$ , a component of the  $^{232}\text{Th}$  decay chain, with  $\beta$  Q-values of 39.52 keV and 25.61 keV, respectively. Due to its low Q-value as well as the relative abundance of  $^{232}\text{Th}$  and their progeny in low background experiments, these observations potentially impact the low-energy background modeling of dark matter search experiments.

*Introduction* – Although numerous astronomical observations support the conclusion that most of the matter in the universe is invisible dark matter, an understanding of its nature and interactions remains elusive [1, 2]. The dark matter phenomenon can be attributed to new particles, such as weakly interacting massive particles (WIMPs) [3, 4]. Tremendous experimental efforts have been mounted to detect nuclei recoiling from WIMP-nucleus interactions, but no definitive signal has yet been observed [5, 6]. This motivates searches for new types of dark matter [7–9] that would induce different experimental signatures in detectors. Several experiments have performed searches for such signatures [10–12].

Typically, these dark matter signals can manifest themselves as an excess of event rates above a known background [11, 13, 14]. Thus, these searches require a precise understanding of the background sources within a detector. As both WIMP dark matter and light-mass

dark matter models predict low energy signals below 10 keV, a precise modeling of the background sources in the low-energy signal regions is crucial. For instance, the recently observed event excess seen by XENON1T [11] can be explained not only by new physics interactions but also by tritium ( $^3\text{H}$ ) contamination, which undergoes a low-energy  $\beta$ -decay (Q-value 18.6 keV, half-life  $t_{1/2} = 12.3$  years).

Because of their long half-lives and large natural abundances, contamination by  $^{238}\text{U}$  and  $^{232}\text{Th}$  as well as their progenies is a significant issue for the low-background dark matter search experiments [15, 16]. Therefore, an accurate understanding of their contamination levels and resultant contributions to detector background is essential for dark matter search experiments. Furthermore,  $^{228}\text{Ra}$ , which is produced by the  $\alpha$ -decay of  $^{232}\text{Th}$ , is of special interest due to the low total Q-value (45.8 keV) of its decay. Based on data from the National Nuclear Data Center [17] and the Nuclear Data Sheet [18],  $^{228}\text{Ra}$  decays to  $^{228}\text{Ac}$  via  $\beta$ -particle emission [19]. Since all  $\beta$ -decays from  $^{228}\text{Ra}$  are to excited states of  $^{228}\text{Ac}$ , the  $\beta$ -particle is always accompanied by a  $\gamma$ -ray as described in Fig. 1.

\* yjko@ibs.re.kr

† hyunsulee@ibs.re.kr

Currently, the lifetimes of the excited states of  $^{228}\text{Ac}$  are unknown [17–19]. Interestingly, the first excited state at 6.28 keV in  $^{228}\text{Ac}$  has  $I^\pi = 1^-$  (where  $I$  is angular momentum and  $\pi$  is parity) while the ground state has  $I^\pi = 3^+$ . The fact that the transition to the ground state is a low-energy transition with a large spin ( $\Delta I = 2$ ) and parity changes suggests that these excited states might actually be metastable isomers with lifetimes on the order of 100 ns ( $\mathcal{O}(100\text{ ns})$ ) [20]. Even though the lifetime of these states have not been previously measured, Ref. [19] pointed out that no coincident 6.67 keV or 6.28 keV  $\gamma$  lines with 13.5 keV or 26.4 keV  $\gamma$  lines were observed. This observation suggests that the 6.67 keV and 6.28 keV states are indeed long-lived isomeric states. If this is the case, the  $\beta$  emission (i.e.  $Q = 39.52\text{ keV}$ ) and the  $\gamma$  emission (i.e.  $Q = 6.28\text{ keV}$ ) will occur at different times and generate different signatures in the detector. However, simulation programs commonly used by dark matter search experiments, such as Geant4 [21], model this decay with the simultaneous emission of the  $\beta$  and  $\gamma$  rays. Failure to account for the  $\mathcal{O}(100\text{ ns})$  lifetime of the metastable state can have a significant impact on the background modeling and interpretation of dark matter search results.

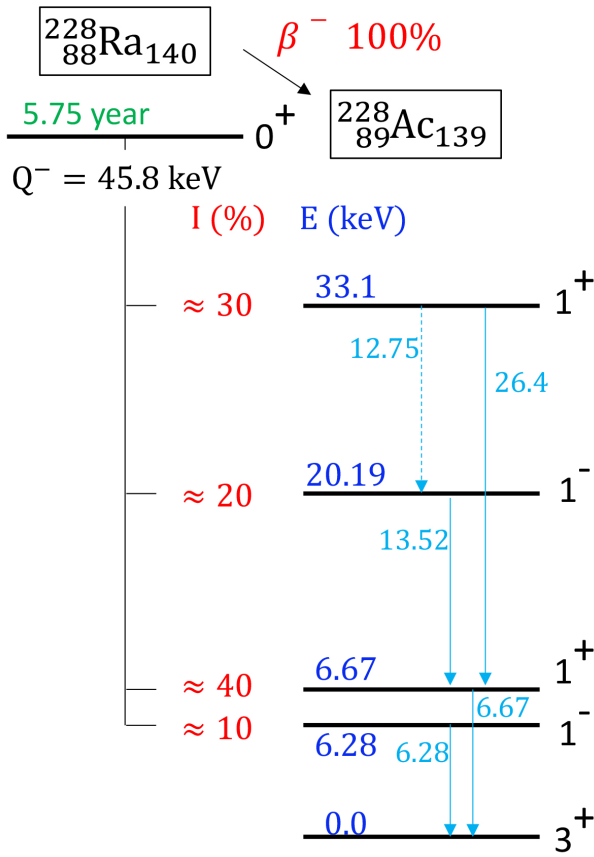


FIG. 1. Nuclear level scheme for  $^{228}\text{Ac}$  adapted from Ref. [19].

In this letter, we report the first observation of new isomeric states in  $^{228}\text{Ac}$  using the COSINE-100 dark matter search detector [22]. The first excited state at 6.28 keV has a  $299 \pm 11\text{ ns}$  lifetime before it transits to the ground state. We have studied how this observation influences the understanding of the background in the low-energy signal region.

*Experiment* – COSINE-100 [22] consists of a 106 kg array of eight ultra-pure NaI(Tl) crystals [23] each coupled to two photomultiplier tubes (PMTs). The crystals are immersed in an active veto detector composed of 2,200 L of a linear alkylbenzene (LAB)-based liquid scintillator (LS) [24, 25]. These eight crystals are referred to as Crystal1 to Crystal8. Crystal1, Crystal5, and Crystal8 are excluded from this analysis due to their high background, high noise rate (Crystal 1), and low light yield (Crystal5 and Crystal8) [26]. The LS is contained within a 3 cm thick shield of oxygen-free copper, a 20 cm thick lead shield, and an array of plastic scintillation counters for muon tagging [27, 28]. Data obtained between 20 October 2016 and 14 April 2020 are used for this analysis with a total exposure of 1181 live days.

Signals from PMTs attached at each end of the crystals are amplified by custom-made preamplifiers: the high-gain anode signal by a factor of 30 and the low-gain signals from the 5th stage dynode by a factor of 100. The amplified signals are digitized by 500 MHz, 12-bit flash analog-to-digital converters (FADCs). A trigger is generated when anode signals with amplitudes corresponding to one or more photoelectrons occur in both PMTs within a 200 ns time window. Both the low-gain dynode and high-gain anode signals are recorded whenever the anode signals produce a trigger. The dynode signals do not produce triggers. The waveforms from the PMTs of all crystals are recorded when the trigger condition is satisfied by at least one crystal. The recorded waveform is 8  $\mu\text{s}$  long starting 2.4  $\mu\text{s}$  before occurrence of the trigger. Detailed descriptions of the COSINE-100 detector and its data acquisition system are provided elsewhere [22, 29].

The energy calibration is performed by tracking internal  $\beta$  and  $\gamma$  peaks from radioactive contaminations in the crystals, as well as by external  $\gamma$  sources [30]. A nonlinear detector response of the NaI(Tl) crystals [31] in the low energy region is observed. An empirical function is used to account for this nonlinearity, as detailed in Ref. [30].

*Data Analysis* – In this analysis, we have studied selected events that contain two distinct pulses, named “two-pulse events”, within our 8  $\mu\text{s}$ -long waveforms. The event selection criteria to remove PMT-induced noise events [32] is applied as a preselection on candidate events. We have developed an offline selection algorithm to identify the two-pulse events using the summed waveforms from the two PMTs of each crystal. The summed waveforms are smoothed by averaging the 30 neighboring time bins into 60 ns bin-width values. We identify two-pulses events as those where, in addition to the initial rising edge of a pulse, there is a second rising edge of at least 1 keV. The application of this requirement on

the leading edge of single-pulse events finds that it is more than 95 % efficient for pulses with energies at approximately 2 keV. However, the selection efficiency of two-pulse events is strongly dependent on both the energies of the two-pulses and the time difference between them ( $\Delta T$ ). Figure 2 shows three examples of the selected two-pulse events that occurred in three different crystals.

Considering two (fast and slow) decay components of the scintillating crystals [33, 34], we characterize each pulse using single rise time ( $\tau_r$ ), two decay times ( $\tau_f$  and  $\tau_s$ ), the starting time of the pulse ( $t_0$ ), and the ratio of the slow-to-fast decay components ( $R$ ):

$$F_i(t) = \frac{1}{\tau_{f_i}} e^{-(t-t_{0_i})/\tau_{f_i}} + \frac{R_i}{\tau_{s_i}} e^{-(t-t_{0_i})/\tau_{s_i}} - \left( \frac{1}{\tau_{f_i}} + \frac{R_i}{\tau_{s_i}} \right) e^{(-t-t_{0_i})/\tau_{r_i}}, \quad (1)$$

Two-pulse events are modeled as  $F(t) = A_1 F_1(t) + A_2 F_2(t)$  where  $A_1$  and  $A_2$  represent the total charge, proportional to the energy, of each pulse. Figure 3 shows the fit results of the two-pulse events where the three events displayed are those from Fig. 2. Here, we can evaluate the energy of the first pulse (E1) proportional to  $A_1$ , the second pulse (E2) proportional to  $A_2$ , and  $\Delta T$  ( $t_{0_2} - t_{0_1}$ ), as well as decay times and pulse shape characteristics of the pulses.

Figure 4 (a) shows a scatter plot of E1 and E2 for the 2–30 keV energy region, where there is a large population of the two-pulse events around E2 equal to about 6 keV. The one dimensional spectrum of E2 is shown in Fig. 4 (b), which presents a two-peak structure with peaks centered at around 6 keV and 20 keV. We model the E2 spectrum as two gaussian functions summed with an exponential background. The mean energies of the two peaks are determined to be:  $6.11 \pm 0.09$  keV and  $20.6 \pm 0.5$  keV, respectively, which closely match the 6.28 keV and 20.19 keV nuclear levels of  $^{228}\text{Ac}$  in Fig. 1.

Figure 4 (c) shows the E1 spectra for E2 values that are greater or less than 13 keV. The E2 spectra have energy distributions with shapes characteristic of  $\gamma$  emissions, while the E1 spectra have broader energy distributions that are characteristic of  $\beta$ -decay and match the decay scheme of  $^{228}\text{Ra}$  into  $^{228}\text{Ac}$  shown in Fig. 1. The data are consistent with the identification of both the 6.28 keV and 20.19 keV excited states of  $^{228}\text{Ac}$  as metastable isomers with lifetimes of  $\mathcal{O}(100\text{ ns})$ . To confirm this hypothesis, we simulate the  $\beta$  spectra of  $^{228}\text{Ra}$  using a Geant4-based simulation which is the same used for background modeling of the COSINE-100 detectors [23, 30]. We model the energy spectra of two  $\beta$ -decays: one with  $Q = 39.52$  keV that decays into the 6.28 keV state and the other with  $Q = 25.61$  keV that decays into the 20.19 keV state. These energy spectra overlaid in Fig. 4 (c) and show good agreement for energies greater than 5 keV. Some discrepancies at low energies are expected due to difficulties in modeling of the selection efficiencies.

Distributions of  $\Delta T$  are shown in Fig. 4 (d) together with results of exponential fits that are used to deter-

mine the lifetime of each transition. Because of significantly lower selection efficiencies in short  $\Delta T$  events, only events with  $\Delta T > 500\text{ ns}$  and  $\Delta T > 300\text{ ns}$  are fitted for the  $E2 < 13\text{ keV}$  and  $E2 \geq 13\text{ keV}$  distributions, respectively. The fitted lifetimes are  $299 \pm 11\text{ ns}$  and  $115 \pm 25\text{ ns}$  for the  $E2 = 6.28\text{ keV}$  and  $E2 = 20.19\text{ keV}$  states, respectively, where only statistical uncertainties are considered.

Because of the large spin and parity changes from the 6.28 keV state to the ground state, the existence of an isomeric state of  $^{228}\text{Ac}$  at 6.28 keV has a straightforward explanation. However, an understanding of the 20.19 keV state as an isomer is not as straightforward because of known decay schemes in literature [17–19] and the measured rate of two-pulse events around 20.19 keV. As one can see in Fig. 1, the 20.19 keV state transits to the 6.67 keV state before decaying to the ground state. To allow for a lifetime of  $\mathcal{O}(100\text{ ns})$  for the 20.19 keV state transition, the 20.19 keV to 6.67 keV transition should have a lifetime of  $\mathcal{O}(100\text{ ns})$ . However, the number of two-pulse events with  $E2 \geq 13\text{ keV}$  is only a few percent of  $E2 < 13\text{ keV}$ . Considering the relative intensities of the  $^{228}\text{Ra}$   $\beta$ -decay shown in Fig. 1, the observed isomeric transition of the 20.19 keV state is only  $\mathcal{O}(1\%)$  of the total  $\beta$ -decay to the 20.19 keV state. This may indicate that the 6.67 keV state is also an isomeric state. In this case, three distinct emissions occur, but not able to be seen in the current analysis efficiently. However,  $\mathcal{O}(1\%)$  events may be accepted as the two-pulse events if the two  $\gamma$  emissions occur too close to be distinguished in the NaI(Tl) crystal. The other possibility is that the 20.19 keV state may transit to the ground state directly with  $\mathcal{O}(1\%)$  branching fraction while the other transitions in the 20.19 keV state are not selected in this analysis. These hypotheses could be studied in detail later with a dedicated experiment.

As a cross-check of the  $^{228}\text{Ac}$  isomer hypothesis, we evaluate the level of  $^{228}\text{Ra}$  contamination in the NaI(Tl) crystals by measuring the rate of the two-pulse events with E2 around 6.28 keV. We select 6.28 keV state events by a requirement of  $E2 < 13\text{ keV}$  in Fig. 4 (b). In order to account for the selection inefficiencies, we performed an extrapolation of the modelings in Fig. 4 (c) and (d) for low-energy and small  $\Delta T$  events. Here, we assume the relative  $\beta$  intensity of the 6.28 keV state as 10 % according to Fig. 1. Table I summarizes the measured  $^{228}\text{Ra}$  activities for the crystals that are compared with the results obtained from the standard background modeling of the COSINE-100 data [30]. The consistency of the results for the  $^{228}\text{Ra}$  contamination supports the interpretation that the observed two-pulse events originate from  $^{228}\text{Ra}$  decays to isomeric excited states of  $^{228}\text{Ac}$ .

*Impact on dark matter searches*— Internal contamination of dark matter detectors by  $^{228}\text{Ra}$  can introduce low-energy events by its  $\beta$ -decay and subsequent  $\gamma$  deexcitation (total Q-value 45.8 keV). Our observation shows that  $Q=39.52\text{ keV}$   $\beta$  and isomeric 6.28 keV  $\gamma$  decays occur with about a 300 ns time difference. We also observed that  $\mathcal{O}(1\%)$  of  $Q=25.61\text{ keV}$   $\beta$  and 20.19 keV  $\gamma$  decays oc-

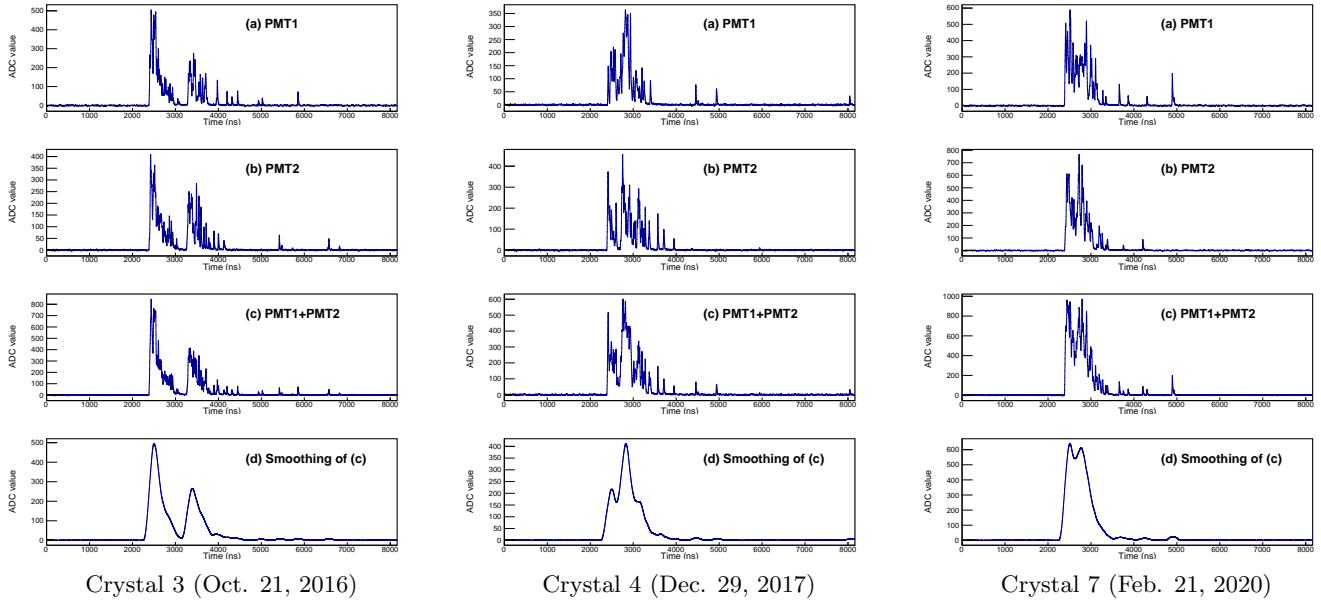


FIG. 2. Examples of selected two-pulse events from different crystals on different dates. (a) and (b) are the signals from the individual PMTs, (c) displays the summed waveform of the two PMT signals, and (d) shows the averaged 60 ns bin signals from the summed waveform. The offline selection of the two-pulse events is performed using the smoothed waveforms.

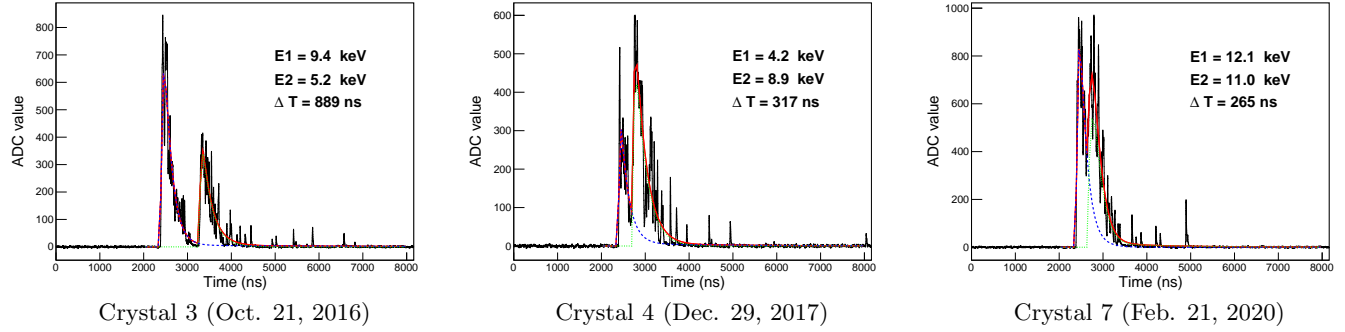


FIG. 3. Results of two-pulse fits for the events in Fig. 2. The energies of each pulse (E1 and E2) and the time difference ( $\Delta T$ ) are listed.

TABLE I.  $^{228}\text{Ra}$  contamination in the COSINE-100 crystals measured using the two-pulse events at 6.28 keV. These measurements are compared with the fit result from the background modeling of the COSINE-100 detector [30].

(mBq/kg)	Two-pulses (this work)	Background modeling
C2	$0.034 \pm 0.010$	$0.032 \pm 0.011$
C3	$0.017 \pm 0.005$	$0.029 \pm 0.010$
C4	$0.024 \pm 0.007$	$0.012 \pm 0.004$
C6	$0.008 \pm 0.002$	$0.024 \pm 0.009$
C7	$0.007 \pm 0.002$	$0.015 \pm 0.006$

cur with about a 100 ns time difference. Our study did not directly observe timing characteristics of the 6.67 keV state, but evidence for the isomeric transition from this

state has been shown in Ref. [19].

Depending on the specific characteristics and data analysis methods of an experiment, the  $\beta$  and  $\gamma$  emissions from  $^{228}\text{Ac}$  could be identified as two separate events due to their  $\mathcal{O}(100\text{ ns})$  time separation. In the case of the COSINE-100 detector, we measure the energy deposited in our detectors by integrating the signal over a  $5\ \mu\text{s}$  time window, resulting in the  $\beta$ -electron and  $\gamma$ -ray being treated as a single event [13, 26]. Therefore, the background modeling using the existing Geant4-based simulation is sufficient for our current analysis [23, 30]. However, if one uses fast response detectors, such as organic scintillators that have a less than 50 ns decay time [35], the coincident  $\beta$  and  $\gamma$  with  $\mathcal{O}(100\text{ ns})$  time difference could be identified as separate events. In the extreme

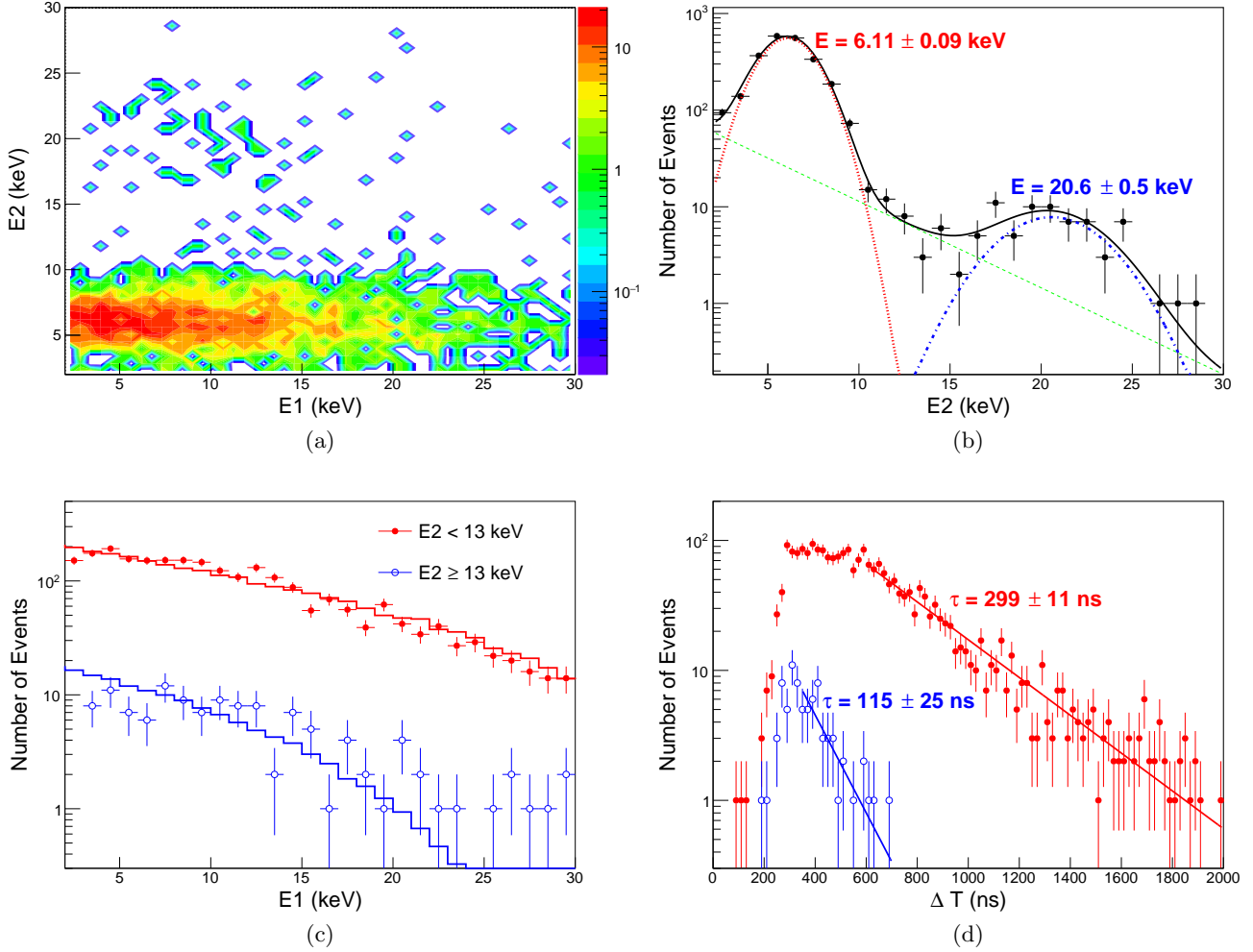


FIG. 4. (a) A scatter plot of energy of the second pulse *versus* the first pulse ( $E_2$  vs  $E_1$ ). (b) The  $E_2$  spectrum (points) is modeled with two gaussians (dotted and dotted-dashed lines) and an exponential background contribution (dashed line). (c) The  $E_1$  spectra for  $E_2 < 13$  keV (filled circles) and  $E_2 \geq 13$  keV (open circles) are compared with a Geant4-based simulation of  $\beta$  spectra with  $Q=39.52$  keV (red solid line) and  $Q=25.61$  keV (blue solid line). (d) The distribution of the two-pulse time difference,  $\Delta T$ , for  $E_2 < 13$  keV (red filled circles) and  $E_2 \geq 13$  keV (blue open circles). Exponential fits (solid lines) to obtain the lifetimes are overlaid.

case, this could result in only the first pulses being properly accounted for while delayed pulses would be ignored because of being too close to the previous event.

We have estimated the impact of these isomeric states of  $^{228}\text{Ac}$  using a Geant4-based simulation, with the result shown in Fig. 5 for three different cases: no isomeric states, two isomeric states at 6.28 keV and 20.19 keV as measured from the COSINE-100 data, and three isomeric states at 6.28 keV, 6.67 keV, and 20.19 keV. Here, we use the energy resolution of the COSINE-100 detector and assume a 100 % detection efficiency. Additionally, we assume identification of only 3% of isomeric decays from the 20.19 keV state. As one can see in the figure, the low-energy spectra are significantly altered if only the  $\beta$  components of the isomeric decays are measured. More specifically, the assumption of a 6.67 keV isomeric state

provides a significantly increased rate in the low-energy signal region. This effect can have a significant impact on dark matter search analyses. For instance, it could potentially contribute to XENON1T excess [11] due to the similar half-life and  $Q$ -values of  $^{228}\text{Ra}$  and  $^3\text{H}$ . The impact of these newly discovered isomer states should be checked by each dark matter search experiment.

*Conclusion*— In conclusion, we have observed new isomers at 6.28 keV and 20.19 keV states in  $^{228}\text{Ac}$  from the  $\beta$ -decay of  $^{228}\text{Ra}$  with the COSINE-100 detector. Their lifetimes are measured to be  $299 \pm 11$  ns and  $115 \pm 25$  ns, respectively. Due to the low  $Q$ -values of these  $\beta$ -decays, these isomeric states have the potential to impact the background modeling of the dark matter search experiments in the low-energy signal region. Thus, a dedicated experiment to measure the nuclear structure of  $^{228}\text{Ac}$  is

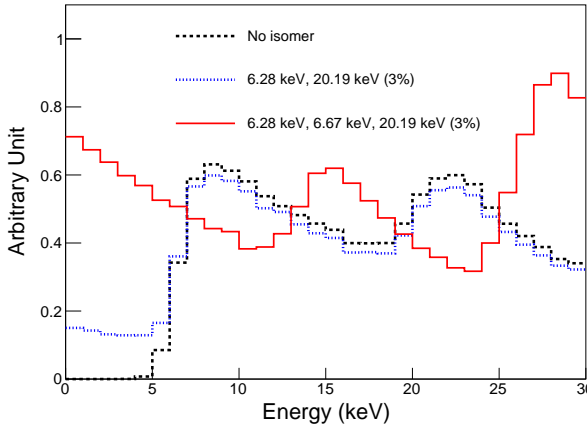


FIG. 5.  $^{228}\text{Ra}$  decay spectra from Geant4-based simulation assuming a few different isomeric states of  $^{228}\text{Ac}$ . Here we assume that only the first pulses from isomeric decays are observed in the detector, considering the resolution of the COSINE-100 detector and 100% selection efficiency. No isomer in  $^{228}\text{Ac}$  (black dashed-line), isomeric states of 6.28 keV and 20.19 keV (blue dotted-line), and 6.28 keV, 6.67 keV, and 20.19 keV (red solid-line) are considered. Here, only 3% identification of isomeric decay of the 20.19 keV state is assumed.

highly desirable.

## ACKNOWLEDGMENTS

We thank the Korea Hydro and Nuclear Power (KHNP) Company for providing underground laboratory space at Yangyang. This work is supported by: the Institute for Basic Science (IBS) under project code IBS-R016-A1 and NRF-2016R1A2B3008343, Republic of Korea; NSF Grants No. PHY-1913742, DGE-1122492, WIPAC, the Wisconsin Alumni Research Foundation, United States; STFC Grant ST/N000277/1 and ST/K001337/1, United Kingdom; Grant No. 2017/02952-0 FAPESP, CAPES Finance Code 001, CNPq 131152/2020-3, Brazil.

---

[1] D. Clowe et al., *A direct empirical proof of the existence of dark matter*, *Astrophys. J.* **648**, L109 (2006).

[2] N. Aghanim et al., (Planck Collaboration), *Planck 2018 results. VI. Cosmological parameters*, *Astron. Astrophys.* **641**, A6 (2020).

[3] B. W. Lee and S. Weinberg, *Cosmological lower bound on heavy-neutrino masses*, *Phys. Rev. Lett.* **39**, 165 (1977).

[4] M. W. Goodman and E. Witten, *Detectability of Certain Dark Matter Candidates*, *Phys. Rev. D* **31**, 3059 (1985).

[5] T. M. Undagoitia and L. Rauch, *Dark matter direct-detection experiments*, *J. Phys. G* **43**, 013001 (2016).

[6] M. Schumann, *Direct Detection of WIMP Dark Matter: Concepts and Status*, *J. Phys. G* **46**, 103003 (2019).

[7] R. Essig, J. Mardon, and T. Volansky, *Direct Detection of Sub-GeV Dark Matter*, *Phys. Rev. D* **85**, 076007 (2012).

[8] D. Kim, K. Kong, J.-C. Park, and S. Shin, *Boosted Dark Matter Quarrying at Surface Neutrino Detectors*, *JHEP* **08**, 155 (2018).

[9] A. Chatterjee, A. De Roeck, D. Kim, Z. G. Moghaddam, J.-C. Park, S. Shin, L. H. Whitehead, and J. Yu, *Search for Boosted Dark Matter at ProtoDUNE*, *Phys. Rev. D* **98**, 075027 (2018).

[10] C. Ha et al., (COSINE-100 Collaboration), *First Direct Search for Inelastic Boosted Dark Matter with COSINE-100*, *Phys. Rev. Lett.* **122**, 131802 (2019).

[11] E. Aprile et al., (XENON Collaboration), *Excess electronic recoil events in XENON1T*, *Phys. Rev. D* **102**, 072004 (2020).

[12] L. Barak et al., (SENSEI Collaboration), *SENSEI: Direct-Detection Results on sub-GeV Dark Matter from a New Skipper-CCD*, *Phys. Rev. Lett.* **125**, 171802 (2020).

[13] G. Adhikari et al., (COSINE-100 Collaboration), *An experiment to search for dark-matter interactions using sodium iodide detectors*, *Nature* **564**, 83 (2018).

[14] K. Abe et al., (XMASS Collaboration), *A direct dark matter search in XMASS-I*, *Phys. Lett. B* **789**, 45 (2019).

[15] H. S. Lee et al., *Development of low-background CsI(Tl) crystals for WIMP search*, *Nucl. Instrum. Meth. A* **571**, 644 (2007).

[16] B. Park et al., (COSINE Collaboration), *Development of ultra-pure NaI(Tl) detectors for the COSINE-200 experiment*, *Eur. Phys. J. C* **80**, 814 (2020).

[17] National Nuclear Data Center, Information based on ENSDF and the Nuclear Wallet Cards, <https://www.nndc.bnl.gov/nudat2/NuDatBandPlotServlet?nucleus=228AC&unc=nds>.

[18] K. Abusaleem, *Nuclear Data Sheets for A=228*, *Nucl. Data Sheets* **116**, 163 (2014).

[19] P. C. Sood, A. Gizon, D. G. Burke, B. Singh, C. F. Liang, R. K. Sheline, M. J. Martin, and R. W. Hoff,  $\beta$  decay of  $^{228}\text{Ra}$  and possible level structures in  $^{228}\text{Ac}$ , *Phys. Rev. C* **52**, 88 (1995).

[20] G. Dracoulis, P. Walker, and F. Kondev, *Review of metastable states in heavy nuclei*, *Rept. Prog. Phys.* **79**, 076301 (2016).

- [21] S. Agostinelli et al., (GEANT4 Collaboration), *GEANT4: A Simulation toolkit*, Nucl. Instrum. Meth. A **506**, 250 (2003).
- [22] G. Adhikari et al., (COSINE-100 Collaboration), *Initial Performance of the COSINE-100 Experiment*, Eur. Phys. J. C **78**, 107 (2018).
- [23] P. Adhikari et al., (COSINE-100 Collaboration), *Background model for the NaI(Tl) crystals in COSINE-100*, Eur. Phys. J. C **78**, 490 (2018).
- [24] J. S. Park et al., (KIMS Collaboration), *Performance of a prototype active veto system using liquid scintillator for a dark matter search experiment*, Nucl. Instrum. Meth. A **851**, 103 (2017).
- [25] G. Adhikari et al., (COSINE-100 Collaboration), *The COSINE-100 Liquid Scintillator Veto System*, [arXiv:2004.03463](https://arxiv.org/abs/2004.03463).
- [26] G. Adhikari et al., (COSINE-100 Collaboration), *Search for a dark matter-induced annual modulation signal in NaI(Tl) with the COSINE-100 experiment*, Phys. Rev. Lett. **123**, 031302 (2019).
- [27] H. Prihtiadi et al., (COSINE-100 Collaboration), *Muon detector for the COSINE-100 experiment*, JINST **13**, T02007 (2018).
- [28] H. Prihtiadi et al., (COSINE-100 Collaboration), *Measurement of the cosmic muon annual and diurnal flux variation with the COSINE-100 detector*, JCAP **02**, 013 (2021).
- [29] G. Adhikari et al., (COSINE-100 Collaboration), *The COSINE-100 Data Acquisition System*, JINST **13**, P09006 (2018).
- [30] G. Adhikari et al., (COSINE-100 Collaboration), *Background modeling for dark matter search with 1.7 years of cosine-100 data*, [arXiv:2101.11377](https://arxiv.org/abs/2101.11377).
- [31] L. Swiderski, M. Moszynski, W. Czarnacki, M. Szawlowski, T. Szczesniak, G. Pausch, C. Plettner, K. Roemer, and P. Schotanus, *Response of doped alkali iodides measured with gamma-ray absorption and compton electrons*, Nucl. Instrum. Meth. A **42** (2013).
- [32] G. Adhikari et al., *Lowering the energy threshold in COSINE-100 dark matter searches*, [arXiv:2005.13784](https://arxiv.org/abs/2005.13784).
- [33] H. Park et al., *Neutron beam test of csi crystal for dark matter search*, Nucl. Instrum. Meth. A **491**, 460 (2002).
- [34] K. W. Kim et al., *Tests on NaI(Tl) crystals for WIMP search at the Yangyang Underground Laboratory*, Astropart. Phys. **62**, 249 (2015).
- [35] P. Sjölin, *The scintillation decay of some commercial organic scintillators*, Nucl. Instrum. Meth. **37**, 45 (1965).